

Chemical Stabilization and Improved Thermal Resilience of Molecular Arrangements: Possible Formation of a Surface Network of Bonds by Multiple Pulse Atomic Layer Deposition

Muriel de Pauli,[†] Matheus J. S. Matos,[†] Pablo F. Siles,^{‡,§} Mariana C. Prado,[†] Bernardo R. A. Neves,[†] Sukarno O. Ferreira,^{||} Mário S. C. Mazzoni,[†] and Angelo Malachias^{*,†}

[†]Departamento de Física, Universidade Federal de Minas Gerais, ICEX, Av. Antonio Carlos, 6627, Belo Horizonte CEP 30123-970, Brazil

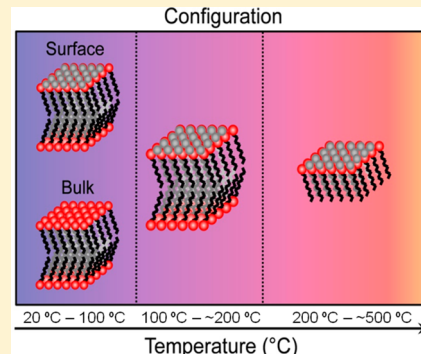
[‡]Material Systems for Nanoelectronics, Technische Universität Chemnitz, 09107 Chemnitz, Germany

[§]Institute for Integrative Nanosciences, IFW Dresden, 01069 Dresden, Germany

^{||}Departamento de Física, Universidade Federal de Viçosa, Av. P. H. Rolfs, sn, Viçosa, Minas Gerais CEP 36571-000, Brazil

S Supporting Information

ABSTRACT: In this work, we make use of an atomic layer deposition (ALD) surface reaction based on trimethyl-aluminum (TMA) and water to modify O–H terminated self-assembled layers of octadecylphosphonic acid (OPA). The structural modifications were investigated by X-ray reflectivity, X-ray diffraction, and atomic force microscopy. We observed a significant improvement in the thermal stability of ALD-modified molecules, with the existence of a supramolecular packing structure up to 500 °C. Following the experimental observations, density functional theory (DFT) calculations indicate the possibility of formation of a covalent network with aluminum atoms connecting OPA molecules at terrace surfaces. Chemical stability is also achieved on top of such a composite surface, inhibiting further ALD oxide deposition. On the other hand, in the terrace edges, where the covalent array is discontinued, the chemical conditions allow for oxide growth. Analysis of the DFT results on band structure and density of states of modified OPA molecules suggests that besides the observed thermal resilience, the dielectric character of OPA layers is preserved. This new ALD-modified OPA composite is potentially suitable for applications such as dielectric layers in organic devices, where better thermal performance is required.



Atomic layer deposition (ALD) has been extensively used to cover inorganic substrates with oxide films. The precise thickness control, the scalable and conformal surface coverage, and the relatively large thermal window make this technique very suited to be used in distinct material classes.¹ Several recent works report the use of organic molecules as substrates or templates to grow distinct oxide films by ALD.^{2–5} The possibility of oxide deposition at low temperatures (even below room temperature) is a crucial parameter to organic systems. The Al₂O₃ is a model system for ALD growth, and its deposition on organic molecules at low temperature is described in the literature in abundance.^{6–9} ALD has also been used as a protective and oxygen barrier layer on plastic substrates, encapsulating layers in organic light-emitting diodes, organic transistors, and organic photovoltaic devices.^{10–15} Also, for organic/inorganic hybrid systems, ALD plays an important role as in p/n junctions of ZnO (n-type) and P₃HT films (p-type) and P₃HT/PCBM solar cells.^{16,17}

Systems of particular interest are tailored organic films and self-assembled molecules with terminal groups designed to be chemically receptive to ALD.^{7,18–20} Density functional theory (DFT) studies reveal chemical routes for the interaction

between the trimethyl-aluminum (TMA), H₂O, and the OH groups (among others) from the molecular heads that are also present in several organic molecules.²¹ This possibility is straightforward for single molecules because in inorganic substrates, the TMA reacts with hydroxyl groups on hydroscopic surfaces. However, the implications and routes for Al₂O₃ growth can be considerably modified in more complex organic environments. In such cases, the description of the deposition process at the molecular level and its consequences on thermal, electric, and optical properties still deserve closer attention because isolated molecules are not the usual scenario with respect to self-organized monolayers and other structural packing.

In this work, we systematically explore indirect evidence of the creation of an artificial composite on the surface of self-assembled multilayers of octadecylphosphonic acid (OPA) [CH₃(CH)₁₇PO(OH)₂] when they are exposed to TMA (the

Received: April 17, 2014

Revised: July 22, 2014

Published: July 23, 2014

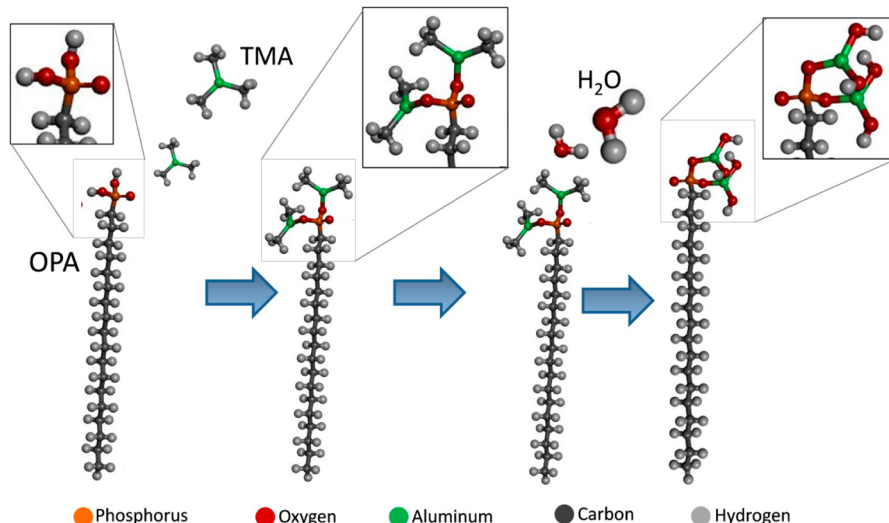


Figure 1. Schematic representation of expected interaction processes between TMA and H_2O with OPA molecules along ALD reactions according to ref 21 (insets show detailed views of the phosphonic group in each expected reaction stage). Initially, TMA molecules interact with OPA phosphonic heads, replacing O–H bonds and leaving methane as the byproduct. Later on, if H_2O molecules are introduced in the chamber, a reaction is expected to take place with CH_3 groups. After one complete TMA/ H_2O cycle, one expects to obtain modified OPA molecules.

Al precursor) molecules, with or without alternating TMA/ H_2O pulses. The OPA molecules are known to form a hexagonally ordered packing along the direction parallel to the surface, as well as a lamellar stack along the perpendicular direction.²² The existence of well-defined configurations, which implies fixed molecular distances, makes this system a suitable choice for the investigation of ALD-induced modifications at the atomic scale. It is found that the obtained structures exhibit improved thermal properties with respect to the original molecules. We show that the mechanisms during each ALD reaction process on a supramolecular surface arrangement, where the chemical potential is spatially modulated, can be different from that observed for a single molecule. The existence of boundaries in such systems may influence the chemisorption, leading to distinct growth behaviors on the same molecular species. X-ray reflectivity (XRR), X-ray diffraction (XRD) measurements, and atomic force microscopy (AFM) were carried out to evidence structural changes in our investigated samples. DFT analysis was also performed, suggesting that experimental results can be properly explained by the formation of an intermolecular bond network.

OPA multilayers were deposited on Si(001) substrates with native SiO_2 by spread coating, as discussed in detail in refs 22 and 23. In all samples, a fixed amount of 1 μL of ethanol solution with a 5 mM OPA concentration was dropped, and the solvent evaporated by mild ultrapure N_2 flux. The obtained multilayers exhibiting large terraces, on the order of hundreds of nanometers, were used as templates to undergo different ALD processes. Series of TMA pulses, designed to modify only the surface termination, as well as TMA/ H_2O cycles, usually done to deposit Al_2O_3 films, were carried out. All processes were made in a Cambridge Nanotech Savannah 100 reactor. The growth temperature was fixed to 59 °C, and pulse and purge time intervals for TMA were set to 0.02 and 20 s, respectively, while the H_2O pulse and purge time were fixed to, respectively, 0.02 and 30 s. Using these parameters on a Si(001)/ SiO_2 substrate, a 0.7 Å/cycle growth rate is obtained whenever TMA and H_2O pulses are alternated.

Different ALD procedures were employed to systematically investigate the chemical bonding of Al atoms and the possibility of formation of Al_2O_3 on the OPA system, as well as their consequences on structural, thermal, and electronic properties. The first ALD procedure consisted of repeating several TMA pulses to induce a complete reaction between this precursor and all available terminations in the phosphonic acid molecules. This step was used as an isolated procedure.²⁴ The second was performed with TMA and H_2O cycles on the OPA samples, the usual Al_2O_3 deposition process. Finally, the third and more complex procedure was done by performing several isolated TMA pulses followed by a number of TMA/ H_2O cycles.

A first sample set (hereafter called the Al-type OPA) was submitted to 100 TMA pulses. A second sample set was obtained by submitting the OPA multilayers to 200 TMA/ H_2O cycles (named here the Ox-type OPA). To complete the scenario, other OPA samples were obtained by performing an initial amount of 100 TMA pulses followed by 50 or 200 cycles of TMA/ H_2O (named the AlOx-type OPA).

AFM measurements were used to map out the sample surface topography before and after the ALD treatment. As reported in previous works,²² OPA multilayers are self-organized in bilayer lamellar steps with a periodicity of 50 Å at the surface (molecule size of 25 Å). XRD and XRR measurements were performed at the XRD2 beamline of the Brazilian Synchrotron Light Laboratory (LNLS – Campinas) in order to observe structural modifications on OPA surface molecules. The beamline is placed after a bending magnet source and is equipped with a cylindrically bent Rh-coated mirror, a sagital focusing Si(111) double-crystal monochromator, and a 4 + 2 axis diffractometer. All measurements were performed with energy fixed of $E = 8$ keV.

Calculations shown here are based on the DFT^{25,26} as implemented in the SIESTA code.^{27,28} For the exchange-correlation potential, we use the generalized gradient approximation (GGA).²⁹ We make use of norm-conserving pseudopotentials in the Kleinman–Bylander factorized form^{30,31} and a double- ζ basis set composed of finite-range numerical atomic pseudofunctions enhanced with polarization

orbitals. A real-space grid is used with a mesh cutoff of 200 Ry. All geometries are optimized so that the maximum force component on any atom is less than 40 meV/Å.

In Figure 1, we show a schematic diagram of Al_2O_3 deposition on the top of an OPA molecule. The first step consists of submitting the OPA molecule to a TMA pulse. As reported in the ref 21, the TMA molecules are expected to bond on OH groups, with the formation of methane as a byproduct. The resulting molecular chemical structure will resemble the configuration depicted in the second panel of Figure 1, still keeping the original oxygen–phosphorus double bond ($\text{P}=\text{O}$) terminations. This configuration is expected for Al-type OPA multilayers. A further step can be implemented pulsing H_2O inside the chamber. The H_2O molecules react with the CH_3 groups in the molecule head. Later, after another TMA pulse, the hydroxyl groups will react, leading to oxygen bonds with the aluminum atoms and, again, the formation of methane. If reactions continue to happen, TMA/ H_2O cycles lead to the deposition of Al_2O_3 on top of phosphonic heads. The rightmost panel in Figure 1 shows what would be expected as surface termination for the Ox-type and AlOx-type OPA multilayers.

AFM images of OPA multilayer substrates are shown in Figure 2a. The lamellar order observed is a result of vertical

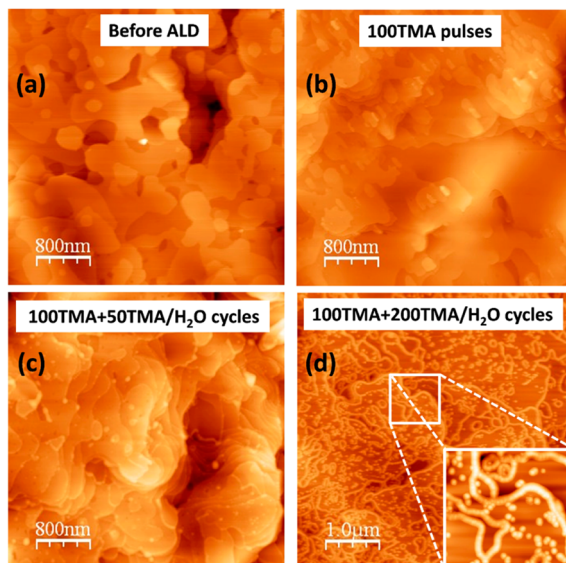


Figure 2. AFM images of (a) OPA multilayers prior to the ALD treatment and (b) OPA multilayers after 100 TMA pulses (Al-type). After TMA reaction procedures identical to those applied in (b), Al_2O_3 is deposited on OPA multilayers with (c) 50 and (d) 200 TMA/ H_2O cycles (AlOx-type samples). The inset in (d) shows a detailed view of the Al_2O_3 deposits at the terrace edges and localized defects. For images (a) and (b), the z scale range is 110 nm, while for (c) and (d), it spans over 135 nm.

packing into bilayer steps, where the phosphonic heads are oriented outward.²³ In Figure 2b, we show an AFM image of the same OPA multilayer after 100 TMA pulses. In such an Al-type sample, the AFM image is not sensitive to possible chemical modifications on the phosphonic heads, although the molecules are expected to have the terminations shown in the second panel of Figure 1. If OPA multilayers are submitted to 100 TMA pulses followed by 50 and 200 TMA/ H_2O cycles, it is possible to observe the formation of Al_2O_3 , although the

grown material does not homogeneously cover the available surface. Such AlOx-type multilayers are shown in Figure 2c,d. In the sample with 100 TMA pulses and 50 TMA/ H_2O cycles, the formation of Al_2O_3 is in an initial state. At this stage, thin lines are detected along terrace steps. In the case of the sample shown in Figure 2d, a larger nominal Al_2O_3 growth thickness is expected at terrace edges (about 150 Å), as denoted by the thicker contours, also seen in detail in the inset. Additionally, punctual deposits are present inside of OPA terraces. Another Ox-type OPA multilayer was also grown, submitted to 200 TMA/ H_2O cycles without the initial series of TMA pulses. The surface morphology is very similar to the sample shown in Figure 2d.

In order to understand the morphological changes at the sample surfaces once TMA/ H_2O cycles are performed, one needs to know first what the reaction for a two-dimensional sheet of OPA (single bilayer) would be. In Figure 3a, we show

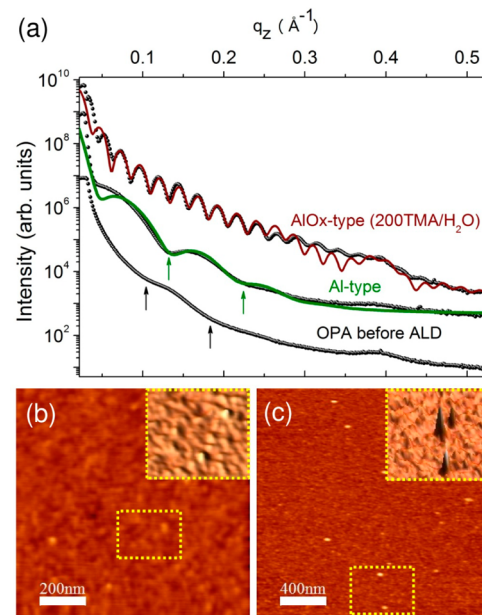


Figure 3. XRR measurements (dots) and kinematical simulations (solid lines) for OPA bilayer samples before and after ALD treatment with TMA and TMA/ H_2O cycles. The lower black dots refer to the XRR data for a bilayer of OPA molecules before the ALD procedure. After 100 TMA pulses, the OPA length increases (middle curve). The upper curve shows the reflectivity profile after 100 TMA pulses followed by 200 TMA/ H_2O cycles (AlOx-type) on OPA bilayer samples. Arrows point to q_z periodicities discussed in the text. The curves were dislocated for better visualization. AFM image of the bilayer sample (b) before ALD treatment and (c) after 100 TMA pulses and 200 TMA/ H_2O cycles. The total z range is 3 nm in (b) and 15 nm in (c). Insets show three-dimensional representations of the topography inside of the highlighted boxes.

the XRR measurements on OPA samples containing only one OPA bilayer before the ALD treatment (lower curve). The reflectivity profile shows interference minima spaced by $\Delta q_z = 0.126 \text{ \AA}^{-1}$, denoting an OPA film thickness of $D = 50 \text{ \AA}$, corresponding to a single OPA bilayer with straight molecules.²² The thickness D is extracted from the q_z interval between successive minima, indicated by arrows in Figure 3a, as $D = 2\pi/\Delta q_z$. In Figure 3b, an AFM image of the OPA bilayer sample before the ALD treatment is shown, with root-mean-square (rms) surface roughness of 1 Å. After 100 TMA pulses,

we observe a modification in the XRR profile (middle curve of Figure 3a), and the bilayer thickness increases to 60 Å due to the $\text{Al}(\text{CH}_3)_2$ groups bound on the phosphonic heads. Although the layer thickness after ALD treatment can be directly retrieved from the q_z interval between minima, a kinematical simulation (solid green line) was used to extract the surface roughness.^{32,33} From this simulation, a 8 Å surface roughness is obtained. Finally, the XRR profile of the AlOx-type sample (upper curve) with 100 TMA pulses followed by 200 TMA/ H_2O cycles shows oscillations corresponding to the deposition of an Al_2O_3 film of 248 Å at OPA-free substrate regions and surface roughness of 6 Å (extracted from the simulation represented by the solid red line). This value is in agreement with the rms surface roughness of 7 Å obtained from the analysis of the AFM image of Figure 3c performed on top of OPA bilayer regions, where localized Al_2O_3 agglomerates only grow on punctual defects at the surface (regions lacking molecules).

The changes in OPA bilayer thickness, depicted in Figure 3, can be considered as a simplification of what would be expected in multilayer systems because the available surface for reaction is smoother, with well-behaved OPA domains. It is crucial to understand whether the TMA reactions take place before the Al_2O_3 formation happens because the formation of oxide agglomerates is only observed at the edges and defects of OPA domains on top of flat terraces. For the investigation of multilayers, it is mandatory to perform XRD, spanning up to higher momentum transfer vectors (larger values of q_z).

XRD measurements on OPA multilayers were carried out by varying the temperature, in order to evidence possible structural modifications that lead to distinct thermal response with respect to untreated OPA stacks.²² A furnace capable of reaching temperatures up to 350 °C was used to perform XRD in situ measurements, which are shown in Figure 4b. Furthermore, ex situ XRD measurements were performed on multilayer samples subjected to higher-temperature treatments of 400, 500, and 600 °C for several minutes. The ex situ results are shown in Figure 4b. In both cases, the samples were kept under a flux of pure N_2 and heated at a rate of 3 °C/min.

We know from previous studies that OPA bilayers remain ordered up to ~100 °C.^{22,34} From room temperature up to approximately 75 °C, three lamellar configurations coexist, each one with a particular tilt with respect to the surface-normal direction. These configurations were thoroughly studied in ref 22 and are schematically represented in Figure 4a. Selected peaks associated with each lamellar packing are labeled in Figure 4b in order to show how pure OPA bulk configurations vanish for temperatures higher than 100 °C. It is also worth mentioning that in-plane hexagonal organization of molecules was found to take place at the surface for temperatures up to 80 °C. The XRD measurements performed in OPA multilayers subjected to all types of TMA/ H_2O treatments discussed here denote an unusually improved thermal stability for the molecules at the surface of each sample.

In Figure 4b,c, we show results on an AlOx-type multilayer sample with 100 TMA pulses, followed by 200 TMA/ H_2O cycles. The curves of Figure 4b show diffraction peaks at room temperature (28 °C), denoting distinct lamellar periodicities due to the coexistence of pure OPA ordered configurations shown in Figure 4a.²² At low q_z conditions, we see interference reflectivity fringes related to Al_2O_3 deposits that are in direct contact with the substrate, with a thickness of 155 Å, in agreement with nominally expected values. As the temperature

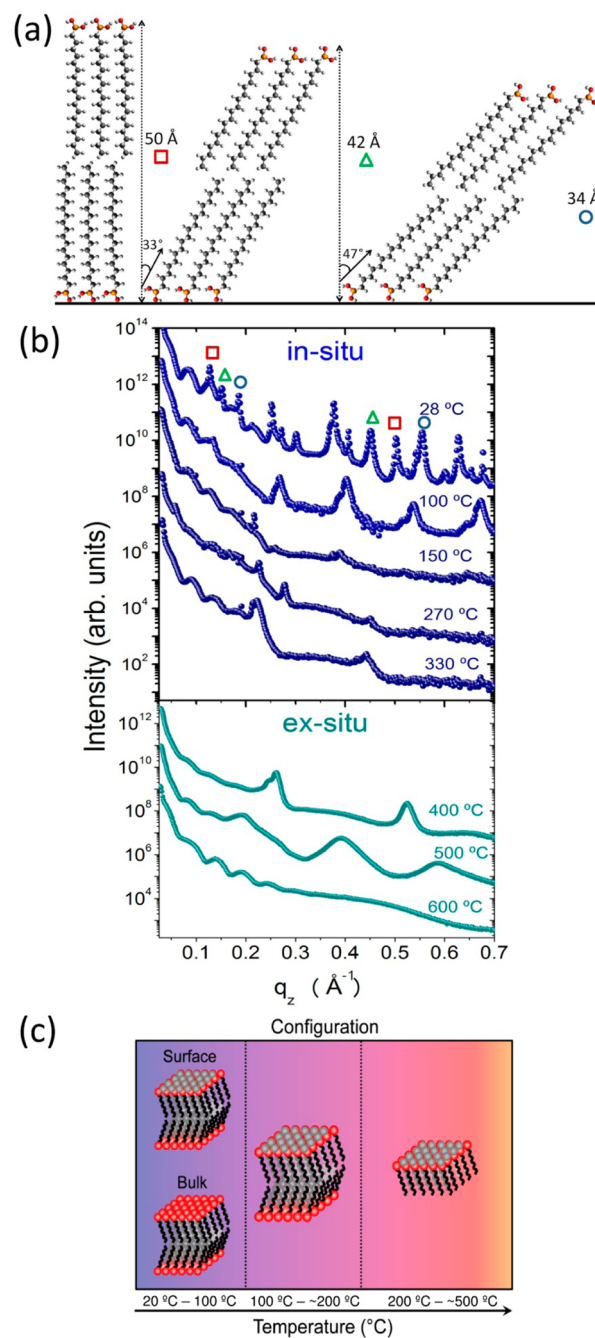


Figure 4. (a) Representation of pure OPA lamellar configurations observed in multilayers according to ref 22. The bilayer height and periodicities retrieved in XRD measurements are due to different supramolecular packing tilts. (b) XRD of AlOx-type OPA multilayers at selected temperatures. At 25 °C, the pure OPA packings are labeled with symbols shown in (a). The upper panel of (b) shows in situ measurements, while the lower panel presents ex situ measurements. The curves were displaced for better visualization. (c) Simplified schematic diagram of ordered OPA configurations as a function of the temperature. Above 100 °C, all pure OPA molecules at the bulk are disordered, and only surface-ordered configurations remain.^{22,34}

increases, all observed diffraction peaks related to pure OPA supramolecular packing vanish. At 100 °C, one sees a considerable difference with respect to pure OPA multilayers. While in a purely organic system no lamellar peak would be expected, after the ALD treatment, we still observe the presence of a periodicity of 46.8 Å that can be ascribed to ordered OPA

bilayers. At 150 °C, the diffraction peaks are barely visible, indicating that ordered regions coexist on a large matrix of molten molecules,³⁴ which came from buried layers that did not bond with the ALD precursors. As the temperature continues to rise, the molten molecules tend to arrange in large droplets,²³ leaving fractions of the surface without any molten agglomerate. At larger temperatures ($T > 200$ °C), we observe the reappearance of diffraction peaks, this time related to a periodicity of 28.6 Å. This periodicity corresponds to the length of a modified OPA molecule. Because, in this case, part of the surface is covered with this molecule type, we believe that platelets of AlOx-type OPA monolayers remain ordered in the 200–500 °C temperature range. The thermal energy above 200 °C is sufficient to break tail–tail interactions, rendering the bilayer configuration unstable. Ex situ XRD measurements are in full agreement with the in situ results. The lower panel of Figure 4b shows that AlOx-type OPA molecules remain ordered up to $T = \sim 500$ °C. At 600 °C, we observe only the reflectivity profile from the pure Al_2O_3 deposits that are thermally stable. The periodicity observed in ex situ measurements at 400 °C is reduced with respect to the periodicity at 330 °C because the XRR measurement is performed at room temperature after the annealing treatment (dilution effects). The temperature evolution of our OPA multilayers was also monitored by in situ AFM heating up to 100 °C, exhibiting lamellar order at this temperature range (see the Supporting Information).

Three distinct regimes can therefore be identified: (i) up to 100 °C, the coexistence of OPA stacked bilayers at the bulk and ALD-modified bilayers at the surface is observed; (ii) from 100 up to ~ 200 °C, one observes the existence of ALD-modified bilayers; (iii) from ~ 200 until ~ 500 °C, ALD-modified monolayers are the only existing type of structure. At higher temperatures, all molecules are in the disordered state. The regimes mentioned above are represented in Figure 4c. It is crucial to mention here that Al-type OPA multilayers have presented the same behavior as that shown in the AlOx-type multilayers of Figure 4b and 4c.

The chemical stability indicated by the absence of Al_2O_3 deposition at the terrace surfaces on AFM images is a crucial point that has to be taken into consideration if one wishes to understand their final atomic configuration. Additionally, the observation of packed molecules by XRD at high temperatures suggests that the interactions among ALD-modified molecules have been changed in the surface layers that interacted with TMA. On pure OPA layers, van der Waals interactions of alkyl chains and hydrogen bonds among phosphonic heads are dominant, but the creation of stronger covalent bonds may be a possible explanation for the observed behavior. We pursued this idea with DFT calculations, aiming to provide a description of possible rearrangements of chemical bonds that would be able to generate a chemically inert and thermally stable structure. Our calculations have pointed to an interesting result in which a two-dimensional covalently bonded compound, organized in a hexagonal lattice, may account for the experimental data reported so far.

The proposed structure, labeled as the terrace surface in Figure 5a, remains with the symmetry and the in-plane structure of pure OPA domains while keeping a very similar in-plane lattice parameter. It has aluminum atoms regularly spaced, with each atom connecting the phosphonic heads of three OPA molecules. In this configuration, all oxygen atoms become bonded to an aluminum atom and a phosphorus atom

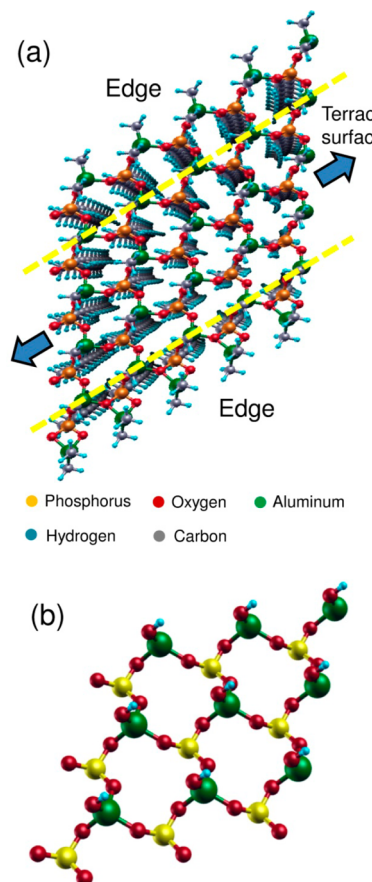


Figure 5. (a) Structure of Al-type OPA terrace surfaces and terrace edges retrieved from DFT calculations. The arrows indicate periodic boundary conditions on the molecule slab used for the DFT simulation of OPA-modified structures. On top of terraces, the covalent network of Al–O–P bonds provides chemical stability against further ALD reactions and improves the thermal resilience of OPA packing. At the edges, the covalent network is discontinued. Two CH_3 groups were found to remain from the reaction with TMA molecules at these positions, allowing the growth of Al_2O_3 after TMA/ H_2O cycles. (b) Detailed representation of the OPA phosphonic heads at the center of the terrace shown in (a) with the Al network of bonds, excluding the alkyl chains for clarity.

at the top of OPA terrace surfaces. Therefore, a possible formation mechanism involves a reaction in which the TMA loses two $-\text{CH}_3$ groups, which, in turn, combine with the two hydrogen atoms from the phosphonic head and leave the system in the form of CH_4 molecules. Actually, our calculations indicate that this reaction is highly exothermic, being favorable by 4.49 eV for each phosphonic head. This value includes a reaction also at the double-bounded oxygen site, not considered in previous DFT calculations.²¹ Such a scenario is mandatory for the formation of the surface network of bonds, which is, in turn, needed to preserve the lamellae of monolayers observed experimentally. The final minimum-energy state is found to be a hexagonal array of OPA molecules with part of the original TMA molecules at the surface; Al atoms bond covalently to three oxygen atoms but keep a single $-\text{CH}_3$ termination at the terrace surface center. Such molecular packing preserves the original OPA in-plane configuration, which is, in this case, constrained to the rigid structure created by ALD deposition. Figure 5b shows a detailed view of the phosphonic heads of the central OPA molecule of Figure 5a (alkyl chains were removed

for clarity), where it is possible to observe the network of bonds that can be created due the insertion of Al atoms from the ALD process.

Now, we may suggest an explanation to depict why Al_2O_3 forms preferentially on terrace edges or on localized defects where molecules are missing. In such regions, the interconnected array is interrupted, leaving Al atoms less coordinated and still bonded to at least two $-\text{CH}_3$ groups, as represented on the edges of Figure 5a. It is to be expected that a further treatment with H_2O will replace methyl groups on Al atoms located at the edges by $-\text{OH}$ groups, keeping the conditions to further Al_2O_3 growth because these are very favorable sites to react with additional TMA molecules. Upon punctual deposition of Al_2O_3 at flat areas of AlOx-type samples, the formation of Al_2O_3 was also observed by AFM. In this case, the presence of a lattice defect (e.g., the absence of a single molecule) is enough to break the surface periodicity. As a consequence, a larger number of $-\text{CH}_3$ terminations becomes available, allowing the appearance of oxide deposits.

On the other hand, in the middle of the structure, a single $-\text{CH}_3$ group is left pointing upward. Because the atomic distances at the modified terrace surfaces will be fixed due to the formation of a rigid structure, a large mismatch or incommensurability between such a lattice and that of the oxide would prevent or render the formation of Al_2O_3 unfavorable for the low deposition temperatures used here. One must recall that OPA molecules present well-defined in-plane ordering along considerably large flat terraces and domains,³⁴ favoring the formation of supramolecular planar arrangements after ALD treatment. It is known that the rigidity of the in-plane packing increases for larger molecule length,³⁵ also playing an important role in the formation of a chemically and thermally stable two-dimensional molecular network. Similar coexistence between reactive and chemically inert sites is found on terraces and edges (defects) of graphene, where growth is achieved only at the edges.^{36,37}

In order to evaluate possible impacts of the ALD-induced modifications on OPA layers used for applications in organic electronic devices, we have carried out a detailed evaluation of the electronic structure of modified and original OPA molecular arrangements. Figure 6a shows that OPA molecules exhibit an insulating character with a well-defined gap of 5.4 eV. After the ALD treatment, molecules at the terrace surfaces still exhibit a similar value for the band gap (5.2 eV), as depicted in Figure 6b. One can, therefore, envisage the use of ALD-modified OPA molecules in organic electronic applications, keeping the original functionality as dielectric layers but with improved thermal resilience, which impacts the operational specifications of devices based on these molecules or similar compounds.

In this work, we have shown that ALD treatment with TMA on long-chain phosphonic acid molecules can produce chemically and thermally stable two-dimensional supramolecular arrangements. XRD measurements directly show that stable configurations can be observed up to 500 °C. For intermediate temperatures, OPA bilayers can coexist with the novel surface artificial composite up to 100 °C. Our simplified configuration diagram shows that OPA bilayers with an upper layer containing Al bonds exist up to 200 °C. DFT calculations were used to investigate the chemical bonds on the treated layers, suggesting the establishment of a two-dimensional stable network on the surface of OPA terraces. In this work, the pre-existing OPA packing has molecular distances that favor the

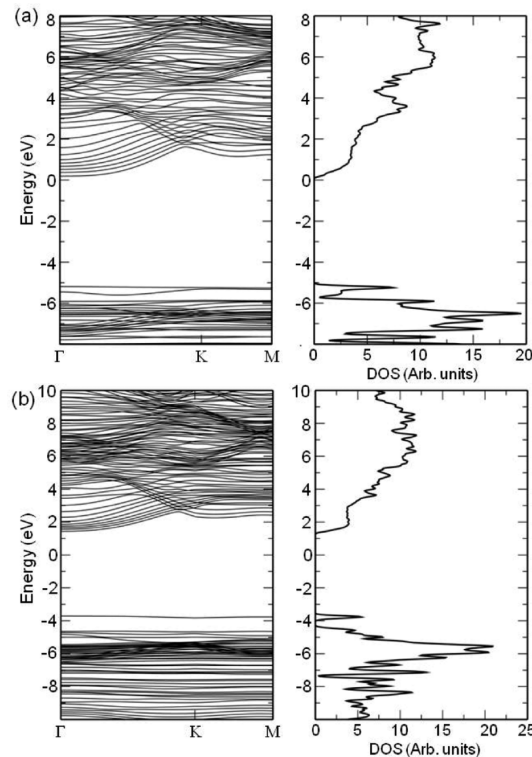


Figure 6. Band structure (left panels) and density of states (right panels) for (a) original supramolecular packing of molecules and (b) modified OPA molecules by ALD treatment (Al-type).

reaction with TMA and consequently the deposition of Al atoms at the surface, with atomic distances close to those of Al_2O_3 . This particular behavior can be explored in a more extended fashion if one correlates ALD reactants that can be used at mild temperatures and molecular arrangements with periodically organized reaction sites where structural conditions for a surface reaction are fulfilled (valence, distances, etc.).

The formation of such a composite material can also be explored for patterning surfaces and preparing them by area-selected deposition processes because edges are reactive while terraces are chemically stable. The TMA-treated molecules may also serve as an organic-to-inorganic transition layer, on top of which depositions that would reorganize the organic molecules can be performed (e.g.: sputtering of metallic layers for contacts). Finally, the band gap of the modified molecular assembly is similar to the value calculated for pure OPA arrangements. This property still makes the system very suitable for applications in dielectric layers, which may require better thermal performances for applications where high power or larger dissipation takes place.

ASSOCIATED CONTENT

S Supporting Information

In situ AFM measurements as a function of the temperature of ALD-modified OPA multilayer samples. This material is available free of charge via the Internet at <http://pubs.acs.org>.

AUTHOR INFORMATION

Corresponding Author

*E-mail: angeloms@fisica.ufmg.br; angelomalachias@yahoo.com. Phone: +(55) 31 3409 6616.

Author Contributions

The manuscript was written through contributions of all authors. All authors have given approval to the final version of the manuscript.

Notes

The authors declare no competing financial interest.

ACKNOWLEDGMENTS

The authors acknowledge the Brazilian Synchrotron Laboratory (LNLS) for the use of the XRD2 beamline, as well as the Brazilian Nanotechnology National Laboratory for the use of atomic force microscopes (MTA group). A.M. is indebted to FAPEMIG Project APQ-01480-12, CAPES pró-equipamentos (UFMG/2011), and FAPESP proposal 2009/09027-3. M.J.S.M. and M.S.C.M. acknowledge INCT - Carbono. B.R.A.N. acknowledges financial support from Fapemig (Project APQ-00379-12) and INCT-NanoCarbono. All authors thank CNPq for funding.

REFERENCES

- (1) George, S. M. Atomic Layer Deposition: An Overview. *Chem. Rev.* **2010**, *110*, 111–131.
- (2) Dube, A.; Sharma, M.; Ma, P. F.; Ercius, P. A.; Muller, D. A.; Engstrom, J. R. Effects of Interfacial Organic Layers on Nucleation, Growth, and Morphological Evolution in Atomic Layer Thin Film Deposition. *J. Phys. Chem. C* **2007**, *111*, 11045–11058.
- (3) Alaboson, J. M. P.; Wang, Q. H.; Emery, J. D.; Lipson, A. L.; Bedzyk, M. J.; Elam, J. W.; Pellin, M. J.; Hersam, M. C. Seeding Atomic Layer Deposition of High-*k* Dielectrics on Epitaxial Graphene with Organic Self-Assembled Monolayers. *ACS Nano* **2011**, *5*, 5223–5232.
- (4) Ferguson, J. D.; Weimer, A. W.; George, S. M. Atomic Layer Deposition of Al_2O_3 Films on Polyethylene Particles. *Chem. Mater.* **2004**, *16*, 5602–5609.
- (5) Peng, Q.; Sun, X.-Y.; Spagnola, J. C.; Hyde, G. K.; Spontak, R. J.; Parsons, G. Atomic Layer Deposition on Electrospun Polymer Fibers as a Direct Route to Al_2O_3 Microtubes with Precise Wall Thickness Control. *Nano Lett.* **2007**, *7*, 719–722.
- (6) Groner, M. D.; Fabreguette, F. H.; Elam, J. W.; George, M. Low-Temperature Al_2O_3 Atomic Layer Deposition. *Chem. Mater.* **2004**, *16*, 639–645.
- (7) Kobayashi, N. P.; Williams, R. S. Two-Stage Atomic Layer Deposition of Aluminum Oxide on Alkanethiolate Self-Assembled Monolayers Using *n*-Propanol and Water as Oxygen Sources. *Chem. Mater.* **2008**, *20*, 5356–5360.
- (8) Lu, P.; Demirkan, K.; Opila, R. L.; Walker, A. V. Room-Temperature Chemical Vapor Deposition of Aluminum and Aluminum Oxides on Alkanethiolate Self-Assembled Monolayers. *J. Phys. Chem. C* **2008**, *112*, 2091–2098.
- (9) Wilson, C. A.; Grubbs, R. K.; George, S. M. Nucleation and Growth during Al_2O_3 Atomic Layer Deposition on Polymers. *Chem. Mater.* **2005**, *17*, 5625–5634.
- (10) Meyer, J.; Görn, P.; Bertram, F.; Hamwi, S.; Winkler, T.; Johannes, H.-H.; Weimann, T.; Hinze, P.; Riedl, T.; Kowalsky, W. $\text{Al}_2\text{O}_3/\text{ZrO}_2$ Nanolaminates as Ultrahigh Gas-Diffusion Barriers—A Strategy for Reliable Encapsulation of Organic Electronics. *Adv. Mater.* **2009**, *21*, 1845–1849.
- (11) Dameron, A. A.; Davidson, S. D.; Burton, B. B.; Garcia, P. F.; McLean, R. S.; George, S. M. Gas Diffusion Barriers on Polymers Using Multilayers Fabricated by Al_2O_3 and Rapid SiO_2 Atomic Layer Deposition. *J. Phys. Chem. C* **2008**, *112*, 4573–4580.
- (12) Yang, Y.-Q.; Duan, Y.; Chen, P.; Sun, F.-B.; Duan, Y.-H.; Wang, X.; Yang, D. Realization of Thin Film Encapsulation by Atomic Layer Deposition of Al_2O_3 at Low Temperature. *J. Phys. Chem. C* **2013**, *117*, 20308–20312.
- (13) Ghosh, A. P.; Gerenser, L. J.; Jarman, C. M.; Fornalik, J. E. Thin-Film Encapsulation of Organic Light-Emitting Devices. *Appl. Phys. Lett.* **2005**, *86*, 223503–3.
- (14) Ferrari, S.; Perissinotti, F.; Peron, E.; Fumagalli, L.; Natali, D.; Sampietro, M. Atomic Layer Deposited Al_2O_3 as a Capping layer for Polymer Based Transistors. *Org. Electron.* **2007**, *8*, 407–414.
- (15) Potscavage, W. J.; Yoo, S.; Domercq, B.; Kippelen, B. Encapsulation of Pentacene C_{60} Organic Solar Cells with Al_2O_3 Deposited by Atomic Layer Deposition. *Appl. Phys. Lett.* **2007**, *90*, 253511/1–253511/3.
- (16) Katsia, E.; Huby, N.; Tallarida, G.; Kutrzeba-Kotowska, B.; Perego, M.; Ferrari, S.; Krebs, F. C.; Guziewicz, E.; Godlewski, M.; Osinniy, V.; et al. Poly(3-hexylthiophene)/ZnO Hybrid pn Junctions for Microelectronics Applications. *Appl. Phys. Lett.* **2009**, *94*, 143501/1–143501/3.
- (17) Malm, J.; Sahramo, E.; Karppinen, M.; Ras, R. H. A. Photo-Controlled Wettability Switching by Conformal Coating of Nanoscale Topographies with Ultrathin Oxide Films. *Chem. Mater.* **2010**, *22*, 3349–3352.
- (18) Li, M.; Dai, M.; Chabal, Y. J. Atomic Layer Deposition of Aluminum Oxide on Carboxylic Acid-Terminated Self-Assembled Monolayers. *Langmuir* **2009**, *25*, 1911–1914.
- (19) Seitz, O.; Dai, M.; Aguirre-Tostado, F. S.; Wallace, R. M.; Chabal, Y. J. Copper–Metal Deposition on Self Assembled Monolayer for Making Top Contacts in Molecular Electronic Devices. *J. Am. Chem. Soc.* **2009**, *131*, 18159–18167.
- (20) Chen, Z.; Sarkar, S.; Biswas, N.; Misra, V. Atomic Layer Deposition of Hafnium Dioxide on TiN and Self-Assembled Monolayer Molecular Film. *J. Electrochem. Soc.* **2009**, *156*, H561–H566.
- (21) Xu, Y.; Musgrave, C. B. A DFT Study of the Al_2O_3 Atomic Layer Deposition on SAMs: Effect of SAM Termination. *Chem. Mater.* **2004**, *16*, 646–653.
- (22) Pauli, M. de; Prado, M. C.; Matos, M. J. S.; Fontes, G. N.; Perez, C. A.; Mazzoni, M. S. C.; Neves, B. R. A.; Malachias, A. Thermal Stability and Ordering Study of Long- and Short-Alkyl Chain Phosphonic Acid Multilayers. *Langmuir* **2012**, *28*, 15124–15133.
- (23) Fontes, G. N.; Moreira, R. L.; Neves, B. R. A. Thermally Induced Stacking of Octadecylphosphonic Acid Self-Assembled Bilayers. *Nanotechnology* **2004**, *15*, 682–686.
- (24) Klepper, K. B.; Nilsen, O.; Hansen, P.-A.; Fjellvag, H. Atomic Layer Deposition of Organic–Inorganic Hybrid Materials Based on Saturated Linear Carboxylic Acids. *Dalton Trans.* **2011**, *40*, 4636–4646.
- (25) Hohenberg, P.; Kohn, W. Inhomogeneous Electron Gas. *Phys. Rev.* **1964**, *136*, B864–B871.
- (26) Kohn, W.; Sham, L. Self-Consistent Equations Including Exchange and Correlation Effects. *J. Phys. Rev.* **1965**, *140*, A1133–A1138.
- (27) Sánchez-Portal, D.; Ordejón, P.; Artacho, E.; Soler, J. M. Density-Functional Method for Very Large Systems with LCAO Basis Sets. *Int. J. Quantum Chem.* **1997**, *65*, 453–461.
- (28) Soler, J. M.; Artacho, E.; Gale, J. D.; García, A.; Junquera, J.; Ordejón, P.; Sánchez-Portal, D. The SIESTA Method for Ab Initio Order-N Materials Simulation. *J. Phys.: Condens. Matter* **2002**, *14*, 2745–2779.
- (29) Perdew, J. P.; Burke, K.; Ernzerhof, M. Generalized Gradient Approximation Made Simple. *Phys. Rev. Lett.* **1996**, *77*, 3865–3868.
- (30) Troullier, N.; Martins, J. L. Efficient Pseudopotentials for Plane-Wave Calculations. *Phys. Rev. B* **1991**, *43*, 1993–2006.
- (31) Kleinman, L.; Bylander, D. M. Efficacious Form for Model Pseudopotentials. *Phys. Rev. Lett.* **1982**, *48*, 1425–1428.
- (32) de Pauli, M.; Malachias, A.; Westfahl, H., Jr.; Bettini, J.; Ramirez, A.; Huang, G. S.; Mei, Y. F.; Schmidt, O. Study of Roughness Evolution and Layer Stacking Faults in Short-Period Atomic Layer Deposited $\text{HfO}_2/\text{Al}_2\text{O}_3$ Multilayers. *J. Appl. Phys.* **2011**, *109*, 063524/1–063524/7.

- (33) Fontes, G. N.; Malachias, A.; Magalhães-Paniago, R.; Neves, B. R. A. Structural Investigations of Octadecylphosphonic Acid Multilayers. *Langmuir* **2003**, *19*, 3345–3349.
- (34) de Pauli, M.; Magalhães-Paniago, R.; Malachias, A. Phase-Dependent Premelting of Self-Assembled Phosphonic Acid Multilayers. *Phys. Rev. E* **2013**, *87*, 052402-1–052402-8.
- (35) Chen, R.; Kim, H.; McIntyre, P. C.; Bent, S. F. Investigation of Self-Assembled Monolayer Resists for Hafnium Dioxide Atomic Layer Deposition. *Chem. Mater.* **2005**, *17*, 536–544.
- (36) Xuan, Y.; Wu, Y. Q.; Shen, T.; Qi, M.; Capano, M. A.; Cooper, J. A.; Yea, P. D. Atomic-Layer-Deposited Nanostructures for Graphene-Based Nanoelectronics. *Appl. Phys. Lett.* **2008**, *92*, 013101-1–013101-3.
- (37) Wang, X.; Tabakman, S. M.; Dai, H. Atomic Layer Deposition of Metal Oxides on Pristine and Functionalized Graphene. *J. Am. Chem. Soc.* **2008**, *130*, 8152–8153.